



Gazi University

**Journal of Science**

PART A: ENGINEERING AND INNOVATION

<http://dergipark.org.tr/gujsa>

# On the Structural, Electric and Optic Properties of $B_{1-x}Al_xN$ Alloys Using Ab Initio Calculation

Özlem BAYAL<sup>1\*</sup> Ali GÜLTEKİN<sup>2</sup> A. Kürşat BİLGİLİ<sup>2</sup> M. Kemal ÖZTÜRK<sup>2</sup>

<sup>1</sup> Photonics Application and Research Center, Gazi University, 06560, Ankara, Türkiye

<sup>2</sup> Department of Physics, Faculty of Science, Gazi University, 06500, Ankara, Türkiye

Keywords	Abstract
$B_{1-x}Al_xN$ Castep Code Structural Properties Elastic Properties Optical Properties	In this study, electronic, optical, elastic, dynamical and structural properties of $B_{1-x}Al_xN$ structure are investigated. During this investigation, density functional theory (DFT) in CASTEP code, local density approximation (LDA) and generalized gradient approximation (GGA) are employed. B/G ratio, Bulk module (B), Scherer module (G), Poisson's ratio ( $\nu$ ), Kellman parameters ( $\xi$ ), Cauchy pressure (P) and compressibility are gained by using elastic constants for the mentioned structure. $B_{1-x}Al_xN$ structure showed epitaxial semiconductor behaviour with well crystallized and brittle characteristics. It also showed cubic structure behaviour for 0.25 and 0.75 Al content and tetragonal structure for 0.50 Al content. With increasing Al ratio, band gap values showed decreasing behaviour as 4.06, 3.56 and 3.34 eV respectively. It is noticed that compressibility is affected by increasing Al contents. It is also found out that real part of refraction constant (RPRF) is in accordance with real part of Dielectric function (RPDF). Peak center of losing function is gained as 27.75 eV for %25 Al content. This value corresponds with maximum Plasmon frequency.
Cite	
Bayal, Ö., Gültekin, A., Bilgili, A. K., & Öztürk, M. K. (2025). On the Structural, Electric and Optic Properties of $B_{1-x}Al_xN$ Alloys Using Ab Initio Calculation. <i>GU J Sci, Part A, 12</i> (1), 619-631. doi:10.54287/gujsa.1646889	
Author ID (ORCID Number)	Article Process
0000-0003-0718-9734	Özlem BAYAL
0009-0004-2381-6368	Ali GÜLTEKİN
0000-0003-3420-4936	A. Kürşat BİLGİLİ
0000-0002-8508-5714	M. Kemal ÖZTÜRK
	<b>Submission Date</b> 26.02.2025 <b>Revision Date</b> 24.03.2025 <b>Accepted Date</b> 10.06.2025 <b>Published Date</b> 30.06.2025

## 1. INTRODUCTION

In recent years, semiconductor devices have a rising trend because of their unique electrical and optical properties. For this reason, II-VI and III-V group compounds are begun to be investigated in detail (Troullier & Martins, 1991; Larbi et al., 2016). Well crystallized triple or quadruple alloys are begun to be used in optoelectronic device production by using different proportions of Boron nitride (BN), Gallium nitride (GaN), Aluminium nitride (AlN), Gallium Phosphate (GaP), Indium nitride (IN), Gallium arsenide (GaAs) (Teles et al., 2002; Riane et al., 2008). Due to their good properties such as wide band gap, mentioned semiconductor devices are commonly used in electronics and optoelectronics (Zheng et al., 2001; Ilyasov et al., 2005; Wu et al., 2007). Improvement of III-nitride technology can contribute constructing light emitting diodes (LEDs), laser diodes (LDs) (Watanabe et al., 2003) and modulation doped field effect transistors (MODFETs) (Zhai et al., 2012; Bouarissa et al., 2013). BN has zinc-blend cubic structure and it is constructed like diamond (Ilyasov

et al., 2005). In terms of technological properties III-Nitride semiconductors are important but they are still not much available for constructing electronic devices and crystallite growth.

Abid et al measured refraction indices and constructed  $B_x Al_{1-x} N$  films which have different Boron concentration by using metal organic vapor phase epitaxy technique (MOVPE) (Matori et al., 2010). Djoidi et al calculated structural and electronic properties of  $B_x Al_{1-x} N$  supercell alloys (Ponomareva et al., 2012).

In this manuscript, main purpose is to improve and adjust critical properties of semi-conductors. For this aim, optical, electronic and dynamic properties of  $B_{1-x} Al_x N$  ( $x$  is Al content) crystallites are examined by using CASTEP package program that is based on DFT.

## 2. MATERIAL AND METHOD

Abid et al measured refraction indices and constructed  $B_x Al_{1-x} N$  films which have different Boron concentration by using metal organic vapor phase epitaxy technique (MOVPE) (Matori et al., 2010). Djoidi et al calculated structural and electronic properties of  $B_x Al_{1-x} N$  supercell alloys (Ponomareva et al., 2012).

In this manuscript, main purpose is to improve and adjust critical properties of semi-conductors. For this aim, optical, electronic and dynamic properties of  $B_{1-x} Al_x N$  crystallites are examined by using CASTEP package program that is based on Discrete Fourier Transform (DFT).

In this study, during calculations DFT is employed by using in-plane waves (Rai et al., 2014). Pseudopotentials for B, Al and N are gained from (LDA) that is parametrized by Perdew, Burke, Ernzerhof and Troullier simulation (Shen & Zhou, 2008). Valence electron configurations of B, Al and N atoms are  $2s^2 2p^1$ ,  $3s^2 3p^1$  and  $2s^2 2p^3$ , respectively. In CASTEP package program, plane oscillation functions of valence electrons are described in the base constant of a plane wave. Ecut et al found out that Troullier-Martins norm-pseudopotentials curves should be used to calculate plane-wave energy (Kleinman, 1962). Interrelated spaces between atoms resembles Brillouin zone. Monkhorst and Pack Mesh used a large number of samples to investigate this situation. Wave functions extend in the plane until cut-off kinetic energy value reaches 0.6 keV. Lattice parameters in Brillouin zone are  $6 \times 6 \times 6$  for these samples used. DFT charge densities are calculated numerically as 1  $\mu C$  per atom.

This study is important because, during calculations both LDA and GGA are used. In calculations of electronic and optical properties LDA is used. Elastic coefficients are found by using GGA. If Al content is considered in the structure the methods mentioned above are more convenient.

In these sensitive calculations an optimization should be made. During this optimization, change in energy is taken as  $1 \times 10^{-5}$  eV/A, stress is 0.06 GPa, maximum displacement is 0.011 Å and SCF tolerance is  $2 \times 10^{-6}$  eV per atom. Structural properties of BN and AlN compounds are calculated by assuming that these compounds are in simple cubic structure.

There are eight atoms (four atoms B and four atoms N) in a unit cell of fc cubic structure belonging to BN compound. When Al is doped instead of B, crystallite structure becomes simple cubic for  $B_{0.75}Al_{0.25}N$  and  $B_{0.25}Al_{0.75}N$ . For  $B_{0.5}Al_{0.5}N$  unit cell becomes tetragonal structure. Crystallite structures of  $B_{1-x}Al_xN$  are shown in Figure 1 and in Table 1 with bond length and with increasing x values. If Al content is 0.25 and 0.75, alloys are in simple cubic structure and bond lengths are the same for B-B, N-N, Al-N and B-N compounds. If Al content is 0.5, because  $sp^3$  hybridization is predominant, alloy becomes simple tetragonal. In Figure 1 bond structure can be seen.

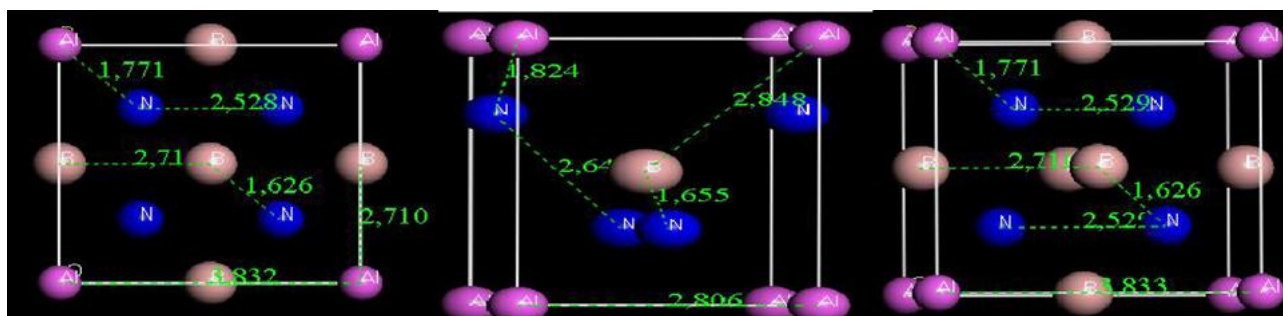


**Figure 1.** Bond length for cubic ( $B_{0.75}Al_{0.25}N$  and  $B_{0.25}Al_{0.75}N$ ) and tetragonal ( $B_{0.50}Al_{0.50}N$ ) of  $B_{1-x}Al_xN$  alloys.

**Table 1.** Crystallite structures and bond length for cubic ( $B_{0.75}Al_{0.25}N$  and  $B_{0.25}Al_{0.75}N$ ) and tetragonal ( $B_{0.50}Al_{0.50}N$ ) of  $B_{1-x}Al_xN$  alloys.

$B_{1-x}Al_xN$	Space group-Structure	B-B(Å)	N-N(Å)	Al-N(Å)	B-N(Å)
$B_{0.75}Al_{0.25}N$	P-43M Primitive cubic	2.48	2.61	4.26	4.1
$B_{0.5}Al_{0.5}N$	P-42M Primitive Tetragonal	2.64	2.64	4.31	4.31
$B_{0.25}Al_{0.75}N$	P-43M Primitive cubic	2.5	2.67	4.4	4.28

By using DFT, lattice constant, cell volume and band gaps are calculated dependent on increasing x in  $B_{1-x}Al_xN$  structure. Experimental and theoretical values are shown in Table 2. Lattice constants for  $B_{1-x}Al_xN$  are calculated as follows dependent on increasing x values:  $x=0.25$ ,  $a=3.79$  Å,  $x=0.50$ ,  $a=2.78$  Å,  $x=0.75$ ,  $a=4.15$  Å. Lattice parameters and Bulk modulus values are in good accordance with previously performed values. Band structures and band gap values are also alike with theoretic values (Wooten, 1972; Godlewski et al., 1995).

As shown in Figure 2, Density of states (DOS) and band structures in first Brilloune zone are calculated in equilibrium state for  $B_{1-x}Al_xN$  structure using lattice coefficients. Results show that DOS and band structures correspond with each other. As seen in Figure 2, energy values show continuous behaviour. DOS curves in bands have sharp peaks. All structures have direct band transition and exhibit semi-conductor behaviour (Khenata et al., 2006; Hosseini, 2008).

Quadratic elastic coefficients are calculated numerically by using “volume conserving” method. 6 independent constants for tetragonal structure are “ $C_{ij}(C_{12}, C_{13}, C_{33}, C_{11}, C_{44}$  and  $C_{66})$ ”. These coefficients must maintain “Born-Huang” criteria for optimization of calculations.

**Table 2.** Lattice constants, bulk modulus and forbidden band gap values for  $B_{1-x}Al_xN$  alloys.

$B_{1-x}Al_xN$	$a_0$ (Å)	$b_0$ (Å)	$c_0$ (Å)	B (GPa)	$E_g$ (eV)
$B_{0.75}Al_{0.25}N$	3.89 <sup>a</sup> ,			317 <sup>a</sup> ,	4.06 <sup>a</sup> ,
(cubic)	3.78	3.75 <sup>b</sup> 3.84 <sup>c</sup> ,	3.78	318 <sup>c</sup> ,	4.9 <sup>e</sup> ,
		3.86 <sup>d</sup>		296 <sup>e</sup>	4.05 <sup>f</sup>
$B_{0.5}Al_{0.5}N$	4.04 <sup>a</sup> ,			266 <sup>a</sup> ,	3.63 <sup>a</sup> ,
(tetragonal)	2.7	3.97 <sup>b</sup> , 4.04 <sup>c</sup> ,	2.7	266 <sup>c</sup> ,	4.4 <sup>e</sup> ,
		4.06 <sup>d</sup>	4.06	245 <sup>e</sup>	3.64 <sup>f</sup>
$B_{0.25}Al_{0.75}N$	4.20 <sup>a</sup> ,			230 <sup>a</sup> ,	3.48 <sup>a</sup> ,
(cubic)	4.14	4.18 <sup>b</sup> , 4.20 <sup>c</sup> ,	4.14	235 <sup>c</sup> , 214 <sup>e</sup>	3.7 <sup>e</sup> , 3.4 <sup>f</sup>

[a, b, c, d, e, f; Troullier, Watanabe, Larbi, Khenata, Woonten, Godlewski]

3 independent coefficients for cubic crystallites are “ $C_{ij}$  ( $C_{12}$ ,  $C_{11}$ , and  $C_{33}$ )”. These must maintain Born-Huang criteria for stability “(( $C_{11}>0$ ,  $C_{11}-C_{12}>0$ ,  $C_{44}>0$  and  $2(C_{11}+C_{12})>0$ )” (Dulong & Petit, 1819) found elastic coefficients for  $B_{1-x}Al_xN$  alloys are calculated numerically by using DFT code. Six number of elastic coefficients are gained for  $B_{1-x}Al_xN$  tetragonal and cubic structures. Calculated elastic coefficients provide each stability conditions in Table 3 (Frantsevich, 1982).

Sherar, Bulk, Young modules, compressibility, B/G, Poisson’s ratio ( $\nu$ ) and cauchy pressure values are calculated by using numerical elastic coefficients. Numerically calculated results for cubic  $B_{0.5}Al_{0.5}N$  are shown in Table 4. B/G and Poisson’s ratio values are important for gaining knowledge about stiffness and durability of material (Born & Huang, 1996). If B/G is bigger than 1.75, structure is elastic. If it is smaller than 1.75, it is brittle (Fox, 2010). If Bulk module is gained large, this means, structure is less compressible (Wooten, 1972). If Cauchy pressure (P) is negative, directional bond is dominant in the structure, if it has positive value metallic bond is dominant. P is generally positive for elastic materials and negative for brittle materials. Poisson’s ratio is a measure of compressibility. If  $\nu$  is near to  $\frac{1}{2}$ , it means the material has tendency to incompressible property.  $\nu$  can also be used for flexibility. If  $\nu$  is bigger than  $\frac{1}{3}$  material shows elastic property. If it is smaller than  $\frac{1}{3}$  it means material is brittle. 0.25 and 0.5 are up and down limits for  $\nu$  for solids. If  $\xi$  is zero this means atom remains in center of tetragonal structure. If  $\xi=1$  then only bond twist is observed the first case, if an atom settles in the center of the tetrahedral structure, the tetrahedral crystallite structure deforms due to structural defects. In the second case, bond buckling defects are more dominant (Fox, 2010).

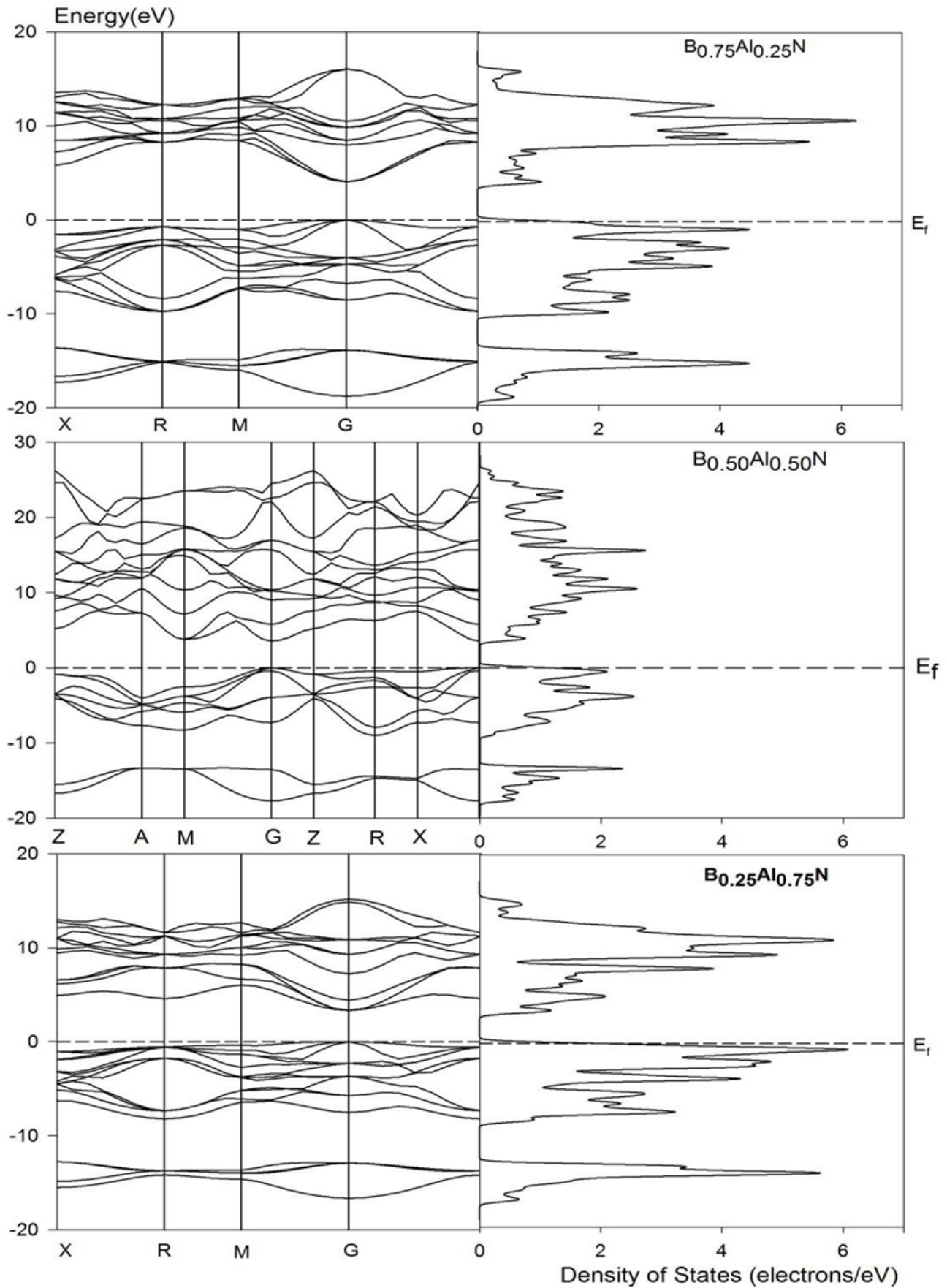


**Figure 2.** Band structure, band energy, forbidden band gap and state density function corresponding to high symmetry points at the Fermi energy level for  $B_{1-x}Al_xN$  alloys.

**Table 3.** The calculated elastic constants (GPa) for  $B_{1-x}Al_xN$ .

$B_{1-x}Al_xN$	$C_{11}$	$C_{12}$	$C_{13}$	$C_{33}$	$C_{44}$	$C_{66}$
$B_{0.75}Al_{0.25}N$ (cubic)	588.1	195.8			308.6	
	600	39.2			236.7	
$B_{0.5}Al_{0.5}N$ (Tetragonal)	555 <sup>g</sup> (cubic)	176.5 <sup>g</sup> (cubic)	178.4	525.3	329 <sup>g</sup> (cubic)	116.6
$B_{0.25}Al_{0.75}N$ (cubic)	373.1	172.1			223.9	

[g; Frantsevitch]

**Table 4.** The estimated  $\nu$ ,  $B$ ,  $G$ ,  $B/G$ , Compressibility,  $\xi$  and  $P$  values for  $B_{1-x}Al_xN$ .

$B_{1-x}Al_xN$	$\nu$	Bulk B (GPa)	Sherar G (GPa)	B/G	Compressibility (1/GPa)	Kleinman par. $\xi$	P (GPa)
$B_{0.75}Al_{0.25}N$ (cubic)	0.24	326.5	251.05	1.3	0.0030	0.48	-112.8
$B_{0.5}Al_{0.5}N$ (tetragonal)	0.28	278.9	186.9	1.5	0.0035	-	-197.5
$B_{0.25}Al_{0.75}N$ (cubic)	0.31	239.1	150.2	1.6	0.0042	0.59	-51.8

When the material is exposed to photon, photon interacts with electron of material. If energy of photon is equal to one of energy gap of the material electron is excited to outer energy levels. If energy of the photon is less than forbidden energy gap photon is not absorbed in the material and this material is transparent for this photon. Absorption and emission of photons cause transitions between energy levels.

$\epsilon_2(w)$  is known as imaginary part of Dielectric function and is calculated by selection rule of wave functions and matrice components of momentum.  $\epsilon_1(w)$  is the real part of Dielectric function and is related to Kramers-Kronig function.

Other optical properties such as, refraction indice  $n(w)$ , absorption and extinction coefficients and function of energy loss  $L(w)$  are derived from imaginary part of Dielectric function. Equations for Dielectric function, refraction indice, absorption and extinction coefficients and energy loss  $L(w)$  are given below (Wooten, 1972).

$$\epsilon_1(w) = 1 + \frac{2}{\pi} \int_0^{\infty} \frac{\epsilon_2(w') w' dw'}{w'^2 - w^2} \quad (1)$$

$$\epsilon_2 = \frac{ve^2}{2\pi\hbar m^2 w^2} \int d^3k \sum_{mn'} [\langle kn, p, kn' \rangle] 2f(kn)x[1 - f(kn')] \partial(E_{kn} - E_{kn'} - \hbar w) \quad (2)$$



Here  $\hbar\omega$  is the energy of incident photon,  $p$  is momentum operator,  $\frac{\hbar}{i} \frac{\partial}{\partial x}$ ,  $kn >$  is an eigenvalue of the energy with wave function  $E_{kn}$  and  $f(kn)$  is Fermi dispersion function.

$$n(\omega) = \frac{1}{\sqrt{2}} \left[ \sqrt{\varepsilon_1^2(\omega) + \varepsilon_2^2(\omega)} + \varepsilon_1(\omega) \right]^{1/2} \quad (3)$$

$$L(\omega) = \text{Im} \left[ \frac{-1}{\varepsilon(\omega)} \right] = \varepsilon_2(\omega) / \left[ \varepsilon_1^2(\omega) + \varepsilon_2^2(\omega) \right] \quad (4)$$

$$\alpha(\omega) = \sqrt{2\omega} \left[ \sqrt{\varepsilon_1^2(\omega) + \varepsilon_2^2(\omega)} - \varepsilon_1(\omega) \right]^{1/2} \quad (5)$$

Results of calculations gained from these equations are shown in Figure 3, 4, 5, 6. Peak centers of real part of Dielectric function are 8.34, 6.95, 5.8 eV for  $x=0.25, 0.50$  and  $0.75$ , respectively.  $\varepsilon_1(0)$  gives static Dielectric coefficient for Al content values  $x=0.25, 0.50$  and  $0.75$  they are calculated as 4.17, 4.5 and 4.25 eV respectively. We mean dielectric constants corresponding to these energies.

According to doping values, absorption starts at 4.17, 4.50 and 4.25 eV energy values corresponding with imaginary part of dielectric coefficient. Values gained are in agreement with band gap energy and they imply transmission between valence and conduction band. This structure behaves like lucid material up to the value which dispersion value starts to rise. Peak centers for imaginary part of Dielectric coefficients are 11.29, 11.81 and 11.18 eV for  $x=0.25, 0.50$  and  $0.75$  Al contents respectively. These values correspond with inter-band transitions (Wooten, 1972).

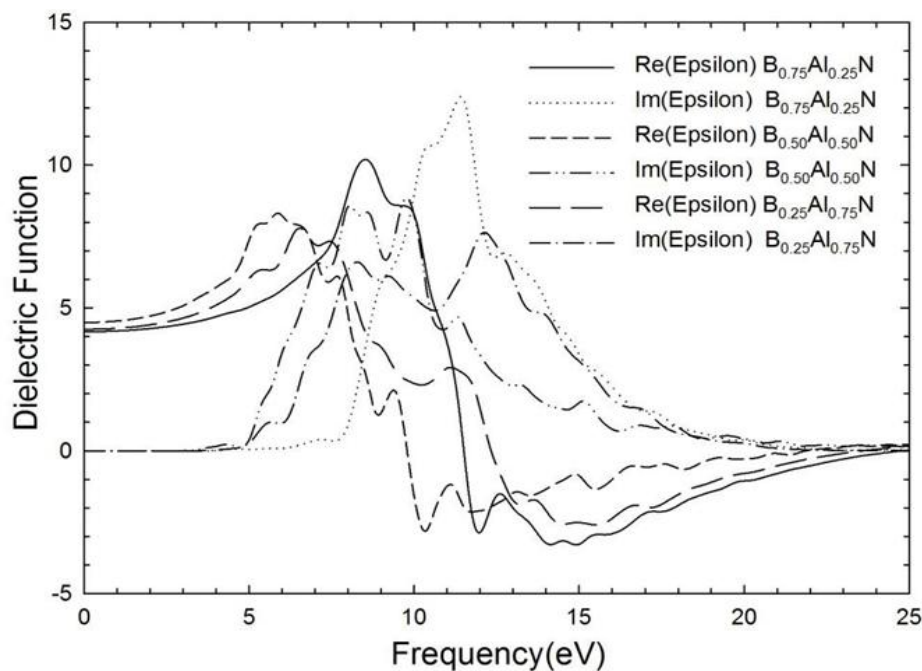


**Figure 3.** The real and imaginary functions of the obtained dielectric function for cubic ( $B_{0.75}Al_{0.25}N$  and  $B_{0.25}Al_{0.75}N$ ) and tetragonal ( $B_{0.50}Al_{0.50}N$ ) of  $B_{1-x}Al_xN$  alloys.

Refraction indices are gained as 2.05, 2.12 and 3.06 for  $x=0.25$ , 0.50 and 0.75 Al contents at  $n(0)$  in accordance with curves of refraction indices. The results gained are in agreement with results of study done by Shunsuke Watanabe et al. (2003). Extinction coefficients are calculated as 4.08 for all three Al content situations. As shown in Figure 4 extinction coefficient values are in agreement with imaginary part of Dielectric coefficient.

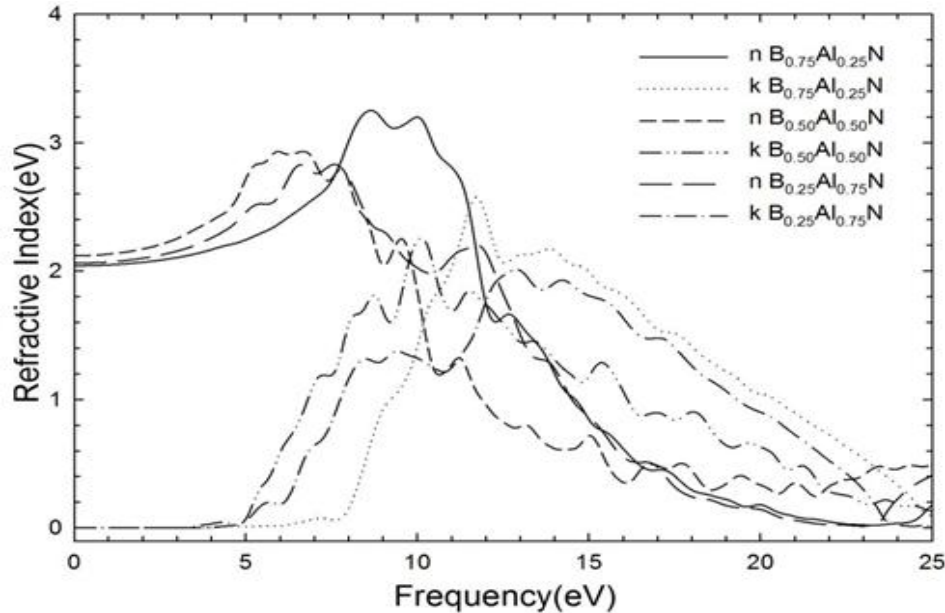


**Figure 4.** Refractive index  $n$  and extinction coefficient for cubic ( $B_{0.75}Al_{0.25}N$  and  $B_{0.25}Al_{0.75}N$ ) and tetragonal ( $B_{0.50}Al_{0.50}N$ ) of  $B_{1-x}Al_xN$  alloys.

For  $B_{1-x}Al_xN$  alloys absorption coefficient values are calculated as 4.09, 3.58 and 3.38 for  $x=0.25$ , 0.50 and 0.75 Al contents, results are shown in Figure 5. At the point which absorption coefficient starts to increase, the imaginary part of dielectric function also starts to increase and are very close to each other. Energy gap at highest absorption occurs at approximately 32.21 eV value.

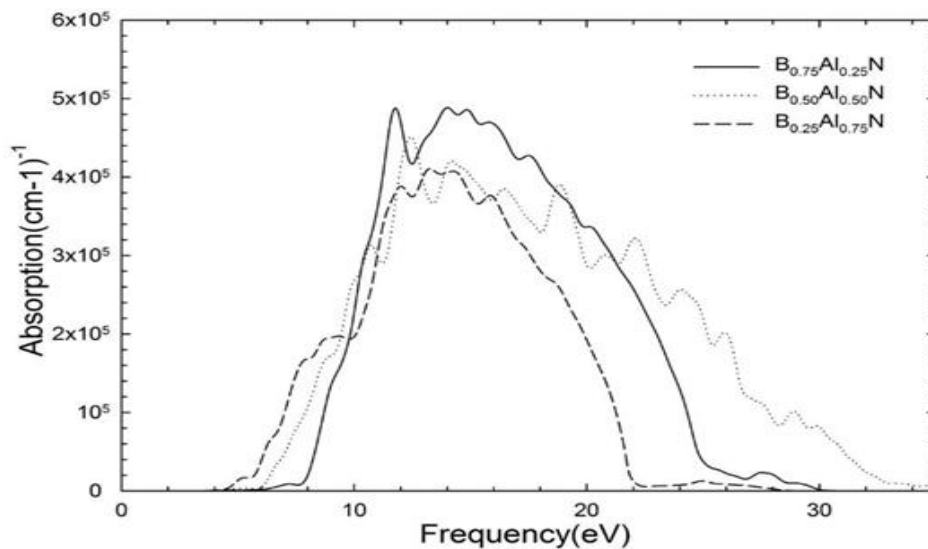


**Figure 5.** Absorption coefficient for cubic ( $B_{0.75}Al_{0.25}N$  and  $B_{0.25}Al_{0.75}N$ ) and tetragonal ( $B_{0.50}Al_{0.50}N$ ) of  $B_{1-x}Al_xN$  alloys.



Energy lose function of the electron is gained from real and complex part of Dielectric function and plot for it is shown in Figure 6. Lose function has variable peaks 21-32 eV energy values. Center of main peak in Losing function is named Plasmon frequency. Where the peak is maximum complex part of Dielectric constant is minimum. Depending on the values of  $x$ , Plasmon frequencies are gained as corresponding to 27.74, 26.60 and 21.76 eV energy values. If the value for Plasmon frequency is bigger than center of peak, samples behave like insulator, if it is smaller, it behaves like metal. Between 0-21 eV values absorption is very low for all three samples. The reason for this situation is that, imaginary part of Dielectric coefficient decays at this energy range (Frantsevich, 1982).

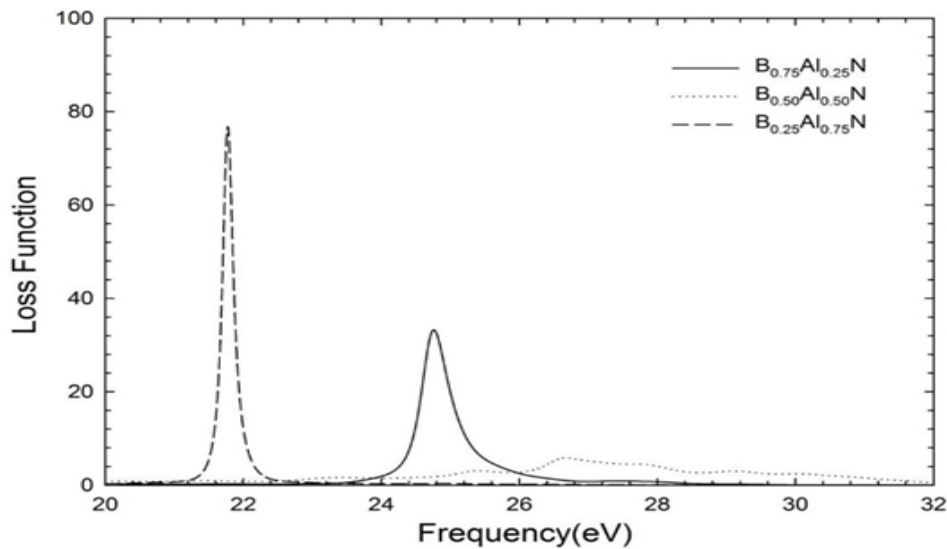


**Figure 6.** Energy Loss Function for cubic ( $B_{0.75}Al_{0.25}N$  and  $B_{0.25}Al_{0.75}N$ ) and Tetragonal ( $B_{0.50}Al_{0.50}N$ ) of  $B_{1-x}Al_xN$  alloys.

Because there are 4 atoms in primitive cell of  $B_{0.75}Al_{0.25}N$  alloy, there are total 12 phonon branches, 3 of them are in acoustic mode and 9 of them are in optics mode. Latitudinal optics (TO) and longitudinal acoustic (LA) phonon modes overlap significantly, so there is no space in phonon dispersion curves and in DOS. For  $B_{0.75}Al_{0.25}N$  alloy, central phonon modes in Brillon zone are found as 18.38, 21.06 and 30.14 THz. Because phonon frequency is not imaginary, this structure is dynamically stable. For this alloy, there are no documents in literature for dispersion curves. All three samples can be accepted as the same family member in terms of phonon frequency. Stable Bulk heat capacity (CV) dependent on temperature is determined by using dispersion and shown in Figure 7 and 8. Starting from low temperature through high temperature CV increase rapidly. For this sample, with increasing temperature CV approaches to conventional asymptotic Dulong-Petit limit. The value of this limit is 1445 Cal/cell. K (Born & Huang, 1996).

### 3. RESULTS AND DISCUSSION

In this study, elastic constants, optical and structural properties of  $B_{1-x}Al_xN$  alloys are investigated by using CASTEP package program based on DFT. Elastic constants for zero pressure, Bulk module, Young module, Sherar module, compressibility, Poisson's ratio ( $\nu$ ) are calculated. Results gained are as follows: B/G ratio less than 1.75 implies samples has brittle property

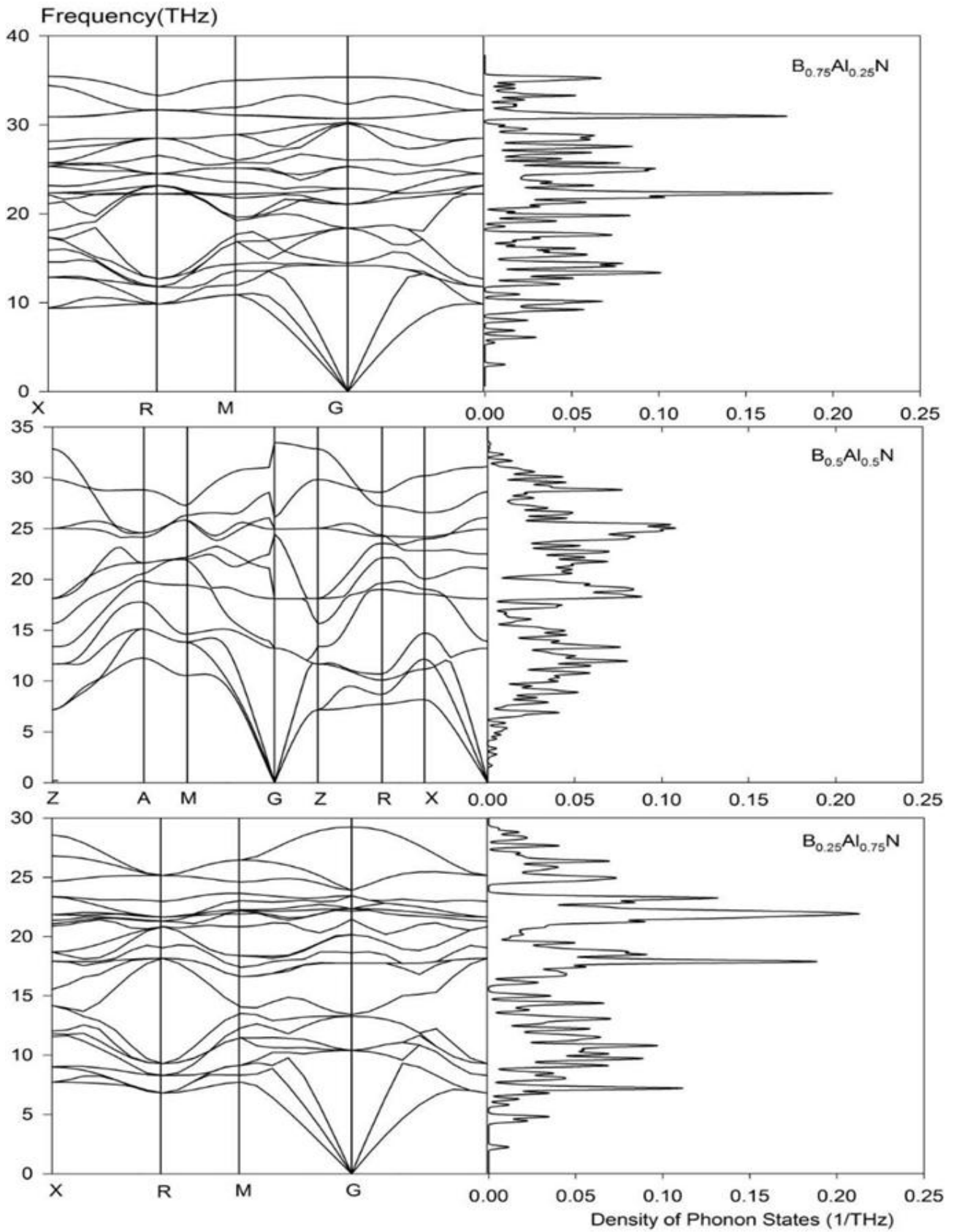


**Figure 7.** Phonon dispersion relation for cubic ( $B_{0.75}Al_{0.25}N$  and  $B_{0.25}Al_{0.75}N$ ) and tetragonal ( $B_{0.50}Al_{0.50}N$ ) of  $B_{1-x}Al_xN$  alloys.

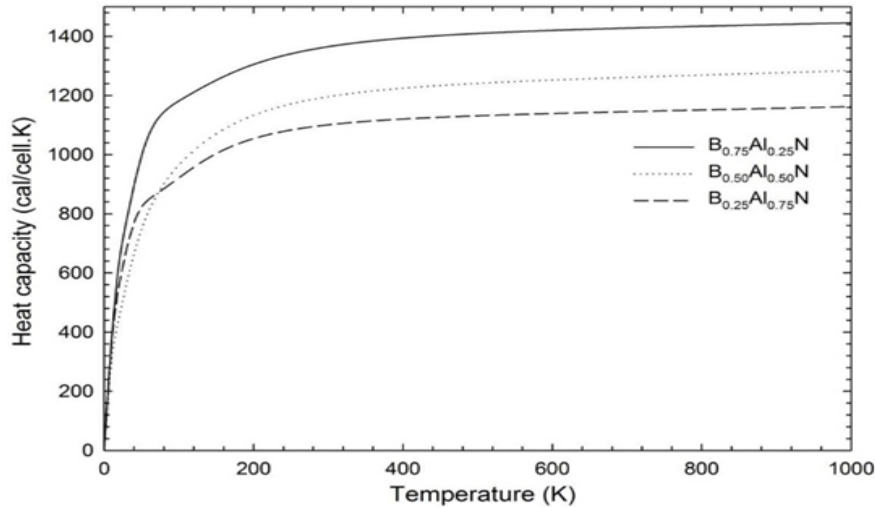


**Figure 8.** Heat capacities for cubic ( $B_{0.75}Al_{0.25}N$  and  $B_{0.25}Al_{0.75}N$ ) and tetragonal ( $B_{0.50}Al_{0.50}N$ ) of  $B_{1-x}Al_xN$  alloys.

#### 4. CONCLUSION

Doping Al instead of B resulted with increasing Poisson's ratio. It is noticed that forces between atoms are mainly central forces and Poisson's ratio values for samples are in the range of 0.25 and 0.5. If Poisson's ratio value is bigger than 1/3 alloy is elastic if not it is brittle. In this study all samples present brittle property. The biggest Bulk module value is found as 326.5 GPa that implies the samples has minimum compressibility. Compressibility value is 0.0030 1/GPa. Its variation dependent on increasing X values is as  $B_{0.75}Al_{0.25}N < B_{0.5}Al_{0.5}N < B_{0.25}Al_{0.75}N$ . Kleinman parameters for  $B_{0.75}Al_{0.25}N$  and  $B_{0.5}Al_{0.5}N$  are as 0.48 and 0.59 respectively. It is not calculated for  $B_{0.25}Al_{0.75}N$  because these samples have tetragonal unit cell. It is seen that in  $B_{1-x}Al_xN$  alloys when Al is doped instead of B, forbidden band gap decreases and metallic property increase. Dielectric coefficients, refractive induce, absorption coefficient and energy loss function are gained by employing Kramer-Kronig equations. All samples present semiconductor behaviour which has transmission of direct band. It is seen that in the increasing values of imaginary part of Dielectric function, they are very close to forbidden band gap. Real part of Dielectric coefficient shows similar properties with refractive indice. Peak center of losing function reaches 27.74 THz value for  $x=0.25$  and this is the highest Plasmon frequency.

#### AUTHOR CONTRIBUTIONS

Corresponding author Ö.B., drawing plots, A.K.B. and A.G., calculations, M.K.Ö., checking and editing, Ö.B.

#### ACKNOWLEDGEMENT

This work was supported by Presidency Strategy and Budget Directorate (Grant Number: 2016K121220).

#### CONFLICT OF INTEREST

The authors declare no conflict of interest.

## REFERENCES

- Born, M., & Huang, K. (1996). *Dynamical theory of crystallite lattices*. Oxford university press.
- Bouarissa, N., & Saib, S. (2013). Elastic modulus, optical phonon modes and polaron properties in  $\text{Al}_{1-x}\text{B}_x\text{N}$  alloys. *Current Applied Physics*, 13(3), 493-499. <https://doi.org/10.1016/j.cap.2012.09.021>
- Dulong, P. L., & Petit, A. T. (1819). *Recherches sur quelques points importants de la theorie de la chaleur*.
- Fox, M. (2010). *Optical properties of solids* (Vol. 3). Oxford university press.
- Frantsevich, I. N. (1982). Elastic constants and elastic moduli of metals and insulators. *Reference book*.
- Godlewski, M., Bergman, J. P., Holtz, P. O., Monemar, B., Bugajski, M., Regiński, K., & Kaniewska, M. (1995). Influence of Growth Conditions on Exciton Properties in Thin Quantum Wells of GaAs/AlGaAs. *Acta Physica Polonica A*, 88(4), 719-722. <https://doi.org/10.12693/aphyspola.88.719>
- Hosseini, S. M. (2008). Optical properties of cadmium telluride in zinc-blende and wurzite structure. *Physica B: Condensed Matter*, 403(10-11), 1907-1915. <https://doi.org/10.1016/j.physb.2007.10.370>
- Ilyasov, V. V., Zhdanova, T. P., & Nikiforov, I. Y. (2005). Electronic energy structure and x-ray spectra of wide-gap AlN and BN crystallites and  $\text{B}_x\text{Al}_{1-x}\text{N}$  solid solutions. *Physics of the Solid State*, 47, 1618-1625. <https://doi.org/10.1134/1.2045343>
- Khenata, R., Bouhemadou, A., Sahnoun, M., Reshak, A. H., Baltache, H., & Rabah, M. (2006). Elastic, electronic and optical properties of ZnS, ZnSe and ZnTe under pressure. *Computational Materials Science*, 38(1), 29-38. <https://doi.org/10.1016/j.commatsci.2006.01.013>
- Kleinman, L. (1962). Deformation potentials in silicon. I. Uniaxial strain. *Physical Review*, 128(6), 2614. <https://doi.org/10.1103/PhysRev.128.2614>
- Larbi, M., Riane, R., Matar, S. F., Abdiche, A., Djermouni, M., Ameri, M., Merabet, N., & Oualdine, A. (2016). Abinitio studies of the structural, electronic, and optical properties of quaternary  $\text{B}_x\text{Al}_y\text{Ga}_{1-x-y}\text{N}$  compounds. *Zeitschrift für Naturforschung B*, 71(2), 125-134. <https://doi.org/10.1515/znbn-2015-0149>
- Matori, K. A., Zaid, M. H. M., Sidek, H. A. A., Halimah, M. K., Wahab, Z. A., & Sabri, M. G. M. (2010). Influence of ZnO on the ultrasonic velocity and elastic moduli of soda lime silicate glasses. *International Journal of Physical Sciences*, 5(14), 2212-2216. <https://doi.org/10.5897/IJPS.9000313>
- Ponomareva, A. V., Isaev, E. I., Vekilov, Y. K., & Abrikosov, I. A. (2012). Site preference and effect of alloying on elastic properties of ternary  $\text{B}_2\text{NiAl}$ -based alloys. *Physical Review B*, 85(14), 144117. <https://doi.org/10.1103/PhysRevB.85.144117>
- Rai, D. P., Ghimire, M. P., & Thapa, R. K. (2014). A DFT study of  $\text{BeX}$  (X= S, Se, Te) semiconductor: modified Becke Johnson (mBJ) potential. *Semiconductors*, 48, 1411-1422. <https://doi.org/10.1134/S1063782614110244>
- Riane, R., Boussahla, Z., Matar, S. F., & Zaoui, A. (2008). Structural and electronic properties of zinc blende-type nitrides  $\text{B}_x\text{Al}_{1-x}\text{N}$ . *Zeitschrift für Naturforschung B*, 63(9), 1069-1076. <https://doi.org/10.1515/znbn-2008-0909>
- Shen, Y., & Zhou, Z. (2008). Structural, electronic, and optical properties of ferroelectric  $\text{KTa}_{1/2}\text{Nb}_{1/2}\text{O}_3$  solid solutions. *Journal of Applied Physics*, 103(7). <https://doi.org/10.1063/1.2902433>

- Teles, L. K., Scolfaro, L. M. R., Leite, J. R., Furthmüller, J., & Bechstedt, F. (2002). Spinodal decomposition in  $B_xGa_{1-x}N$  and  $B_xAl_{1-x}N$  alloys. *Applied Physics Letters*, 80(7), 1177-1179. <https://doi.org/10.1063/1.1450261>
- Troullier, N., & Martins, J. L. (1991). Efficient pseudopotentials for plane-wave calculations. *Physical Review B*, 43(3), 1993. <https://doi.org/10.1103/PhysRevB.43.1993>
- Watanabe, S., Takano, T., Jinen, K., Yamamoto, J., & Kawanishi, H. (2003). Refractive indices of  $B_xAl_{1-x}N$  ( $x=0-0.012$ ) and  $B_yGa_{1-y}N$  ( $y=0-0.023$ ) epitaxial layers in ultraviolet region. *physica status solidi (c)*, (7), 2691-2694. <https://doi.org/10.1002/pssc.200303549>
- Wooten, F. (1972). *Optical properties of solids*. Academic Press.
- Wu, Z. J., Zhao, E. J., Xiang, H. P., Hao, X. F., Liu, X. J., & Meng, J. (2007). Crystallite structures and elastic properties of superhard Ir N 2 and Ir N 3 from first principles. *Physical Review B*, 76(5), 054115. <https://doi.org/10.1103/PhysRevB.76.054115>
- Zhai, H., Li, X., & Du, J. (2012). First-principles calculations on elasticity and anisotropy of tetragonal tungsten dinitride under pressure. *Materials Transactions*, 53(7), 1247-1251. <https://doi.org/10.2320/matertrans.M2011373>
- Zheng, J. C., Wang, H. Q., Huan, C. H. A., & Wee, A. T. S. (2001). The structural and electronic properties of  $(AlN)_x(C_2)_{1-x}$  and  $(AlN)_x(BN)_{1-x}$  alloys. *Journal of Physics: Condensed Matter*, 13(22), 5295. <https://doi.org/10.1088/0953-8984/13/22/322>